SUPPLEMENTARY MATERIALS

Tornado-Inspired Acoustic Tweezers for Trapping and Manipulating Microbubbles

Wei-Chen Lo [1], Ching-Hsiang Fan [2,3], Yi-Ju Ho [1], Chia-Wei Lin [1], Chih-Kuang Yeh [1,4,*]

[1] Department of Biomedical Engineering and Environmental Sciences, National Tsing Hua University, Hsinchu, 30013 Taiwan

[2] Department of Biomedical Engineering, National Cheng Kung University, Tainan, Taiwan

[3] Medical Device Innovation Center, National Cheng Kung University, Tainan, Taiwan

[4] Institute of Nuclear Engineering and Sciences, National Tsing Hua University, Hsinchu, Taiwan

This PDF file includes:

Method

Table S1 to S3

Figures S1 to S8

Legends for movies S1 to S9

Other supplementary materials for this manuscript include the following:

Movies S1 to S9

Method

Transducer characterization

The transducer was constructed based on a previous piezocomposite array structure (1). A single concave PZT substrate (ELECERAM, Taiwan) was carved into four sectors with a 2-mm kerf on the back electrode using a laser cutter. To ensure that the PZT did not block the light path of the microscope, a 3-mm aperture was drilled through it. Four coaxial wires (signal and ground) were attached to the PZT, and sealed in a polylactic acid cylindrical case printed using a three-dimensional (3D) printer (ATOM 2.5 FX, ATOM, Taiwan). Two arbitrary-waveform generators (AFG3022C, Tektronix, USA) synchronized to a phase difference of 2π radians at 3 MHz drove the transducer at peak negative pressures of 80–800 kPa and duty cycles of 3–30%. The spatial distribution and peak negative pressure of the AVT were measured by an 85-μm needle hydrophone (HGL-0085, ONDA, USA) mounted on a 3D computer-controlled motor system. The transducer and hydrophone were submerged in a tank of degassed water kept at 19–21°C.

MB fabrication

The MBs were fabricated by dissolving 1,2-distearoyl-sn-glycero-3-phosphoethanolamine-N-[carboxy(polyethylene glycol)-5000] (DSPE-PEG 5K, Avanti Polar Lipids, USA), 1,2-dipalmitoyl-sn-glycero-3-phosphocholine (DPPC, Avanti Polar Lipids, USA), and 1,2-Distearoyl-sn-glycero-3-phosphoglycerol (DSPG, Avanti Polar Lipids, USA) at a molar ratio of 1.8:1:1.5 in chloroform. After removing the chloroform using an evaporator (R-210, Büchi Labortechnik, Switzerland), 1% glycerol-containing

phosphate-buffered saline was added to the lipid mixture. The gas within the sample was then replaced with C_3F_8. The MBs were formed by intense mechanical shaking by an agitator for 45 s. Finally, to separate unreacted lipids, centrifugation was applied to the MBs at 6,000 rpm (corresponding to 2000×*g*) for 3 min. The morphology of the MBs could be visualized in bright-field microscopy images, while the red fluorescence images of the MBs were observed by embedding DiI into the lipid shell of the MBs. The mean size and concentration of MBs were measured by a particle analyzer (Multisizer 3, Beckman Coulter, USA).

Assessment of the number of AVT-trapped MBs

To estimate the number of trapped MBs by AVT, we performed the MBs trapping procedure in a self-made static chamber for visually counting the trapped MBs via microscopic imaging. The AVT transducer was positioned on top of the chamber and confocally aligned with objective. The static chamber is composed of a metal ring lid, optical-acoustic penetrable plastic wrap, a glass plate, and a metal ring base (Fig. S3(a)). A total volume of 50 μl MBs with different concentrations (20, 40, and 80×10^6 MBs/mL) were added just below the plastic wrap. Note that the MBs concentration was 1/100 lower than that in main text because many MBs were stacked along the z axis when the concentration of MBs was higher than 80×10^6 MBs/mL. The AVT trapping was applied for 1 s. In order to clearly identify the individual MB on objective observing plane, the images were acquired 10 sec after finishing the AVT trapping (Fig. S3(b-c)). The counting of MBs from acquired images was conducted by ImageJ software. Note that we verified only one layer of MBs below the plastic wrap via adjusting the observing plane (i.e., one

more MBs diameter away) relative to the plastic wrap position. During the experiment, a 4× objective was used to verify the successfully trapping and followed a 100× oil objective to count the MBs below the plastic wrap because the depth of field of the 100× oil objective was much smaller than the size of observed MBs (0.8 μm vs. 0.7-8.0 μm). The number of AVT trapped MBs in the main text could be estimated by linear fitting and extrapolation according to Fig. S3(e).

Assessment of AVT trapping and clustering of MBs

The MBs were infused into a 200 μm cellulose tube with flow velocity of 2.6 cm/s (Fig. S4(a)). The AVT trapping (3 MHz, 800 kPa, 30% duty cycle) was performed on MBs with a time interval of 1 s for 3 min (Fig. S4(b)). The pulse repetition frequency (PRF) was regulated to 1 Hz following the flow velocity to confirm that MBs were trapped once within the focal volume of AVT. The waste after AVT trapping was collected and the size distribution of residual MBs was measured by the particle analyzer.

***In vitro* AVT-enhanced drug delivery**

For the drug delivery application of AVT, we hypothesized that the pulses that caused the trapping effects and those that produced fragments of MBs could be used together, in sequence, to improve local drug delivery. AVT pulses can concentrate the surrounding free MBs and fragmentation pulses rupture the MBs as well as spray the cargo of the MBs in the local area. To verify if this AVT method can be used as a drug delivery technology. The experiments were conducted in static chambers based on the system proposed by Shortencarier et al. (2). The static chamber is composed of a metal ring lid, optical-acoustic

penetrable plastic wrap, a glass plate, and a metal ring base (Fig. S5(a)). A total volume of 50 µl MBs solution (concentration: 40×10^6 MBs/mL) was added just below the plastic wrap. Note that the MBs concentration used in this experiment was 1/100 lower (40×10^6 MBs/mL) than that in main text (40×10^8 MBs/mL) because the background fluorescence intensity would be too high to differentiate the released DiI from MBs at the case of high MBs concentration. The AVT transducer was positioned on top of the chamber and confocally aligned with the objective. The acoustical sequences used in this experiment are diagrammed in Fig. S5(b). This sequence of pulses produced trapping force and destroyed MBs. The acoustic parameters of each sequence are listed in Table S1. We expected that the sequence of ultrasound pulses could deflect the MBs toward the glass plate and then disrupt them, releasing their contents onto the glass plate (Fig. S5(c)). For comparison, an acoustic radiation force (ARF) followed by fragmentation group and fragmentation only group were also included. Each plate was exposed for 1 s. After insonation, the intensity and spatial extent of the fluorescence adherent to the glass plates were examined by fluorescence microscopy.

Assessment of AVT-trapping effect on the surrounding RBCs and hemolysis of RBCs

In order to examine the effect of AVT on RBCs, two experiments were performed: (1) observing the morphology; (2) detecting the occurrence of hemolysis after performing AVT trapping. Hemolysis testing is performed based on American Society for Testing and Materials (ASTM) F756, Standard Practice for Assessment of Hemolytic Properties of Materials (3).

RBCs were isolated by centrifugation from whole pig blood and washed with a 0.15 M saline solution. The RBCs were mixed with MB solution and infused into a 200 μm cellulose tube with flow velocity of 2.6 cm/s. The AVT trapping was performed on MBs with a time interval of 1 s for 3 min. The time interval of AVT trapping was regulated to 1 s following the flow velocity to confirm that MBs were trapped once within the focal volume of AVT. The waste after AVT trapping was collected and was then centrifuged for 5 min to separate RBCs from the waste solution. To observe the morphology changes before and after the AVT trapping, the RBCs images were obtained using a 100× oil objective. The occurrence of RBCs lysis after AVT trapping process was verified by detecting the amount of hemoglobin with a spectrophotometer (Tecan Infinite M200, Tecan Trading AG, Männedorf, Switzerland) at an absorbance wavelength of 541 nm.

Assessing AVT-trapped MBs would occlude the small capillaries or downstream vessels in mice

The MBs were intravenously injected 20 s before starting AVT trapping and the trapping sequence was performed according to the abovementioned trapping sequence *in vivo*. The sequential fluorescence images were acquired for 30 s within two different size vessels (20 μm and 200 μm) at two time points: (1) during the onset of AVT and (2) 60 min after AVT trapping. A region of interest (20 μm vessel: 20 μm diameter circle; 200 μm vessel: 200 μm diameter circle) downstream of AVT-trapped MBs was selected to assess the change in fluorescence intensity within the vessel. The residues high fluorescence intensity after AVT-trapping could be referred to vessel occlusion the vessel. In contrast, the vessel had relatively low fluorescence intensity indicating unblock of vessel.

Assessment of AVT safety *in vivo*

To assess the safety of AVT trapping, we traced the electrocardiogram (ECG), heart rate, body temperature, blood oxygen concentration, and potential toxicology of mice before, during, and after receiving AVT trapping. Before starting the experiments, the healthy animals were randomly divided into two groups: (1) AVT trapping + MBs (N=3); (2) healthy mice without AVT trapping (N=3). The MBs were intravenously injected 20 s before trapping and the AVT trapping was performed with time interval of 1 s for 3 min. The time interval of AVT trapping was regulated to 1 s following the flow velocity to confirm that MBs were trapped once within the focal volume of AVT. The ECG, heart rate, body temperature, and blood oxygen concentration measurements were monitored in real time for 5 min by Physiosuite (Kent Scientific, CT, USA).

Assessment of the integrity of AVT waveform would remain intact after penetrating homogeneous tissue

We investigated if the waveform of AVT was decorrelated as it passed through whole brain of mice via the hydrophone. The mice brain was fix in an agarose phantom (2%) to maintain the position between the hydrophone and the transducer (Fig. S8(a-b)). The spatial distribution and peak negative pressure of the AVT with and without penetrating mice brain were measured by the hydrophone with the 3D computer-controlled motor system. The transducer and hydrophone were submerged in a tank of degassed water kept at 19–21°C.

Table S1. The summarized acoustic parameters of applied sequences.

	AVT	Radiation force	Fragmentation
Frequency (MHz)	3	3	3
Acoustic pressure (kPa)	160	160	1600
PRF (Hz)	9000	9000	Single pulse
Cycle number	100	100	5
Duty cycle (%)	30	30	Single pulse

Table S2. Whole blood analysis.

Factors	Healthy mice	AVT + MBs
*ALP (U/L)	83 ± 3.6	83.3 ± 3.9
*ALT (U/L)	44.7 ± 6.7	39.8 ± 7.5
*TBIL (mg/dL)	0.4 ± 0.1	0.3 ± 0.1
*ALB (g/dL)	2.1 ± 0.3	2.2 ± 0.1
#CRE (mg/dL)	0.5 ± 0.0	0.5 ± 0.1
#PHOS (mg/dL)	11.1 ± 1.2	7.2 ± 0.4
#BUN (mg/dL)	24.3 ± 2.1	11.5 ± 2.9
#BUN/CRE	48.7 ± 4.2	26.7 ± 8.8
GLU (mg/dL)	316.0 ± 56.2	161.5 ± 23.5
TP (g/dL)	3.8 ± 0.4	4.4 ± 0.8
AMY (U/L)	200.0 ± 24.5	199.5 ± 8.7
GLOB (g/dL)	1.7 ± 0.4	2.3 ± 0.8
ALB/GLOB	1.2 ± 0.3	1.1 ± 0.4

*Liver function, #Kidney function

Table S3. Parameters used for the simulations.

Parameter (unit)	Value
V_0 (m^3)	5.5×10^{-18}
R_0 (m)	1.1×10^{-6}
ω (s^{-1})	$2\pi\times3.1\times10^{-6}$
ω_0 (s^{-1})	$2\pi\times10\times10^{-6}$
P_a (kPa)	800
β_{tot}	0.483
ρ (kg/m^3)	1000
D/T (%)	30

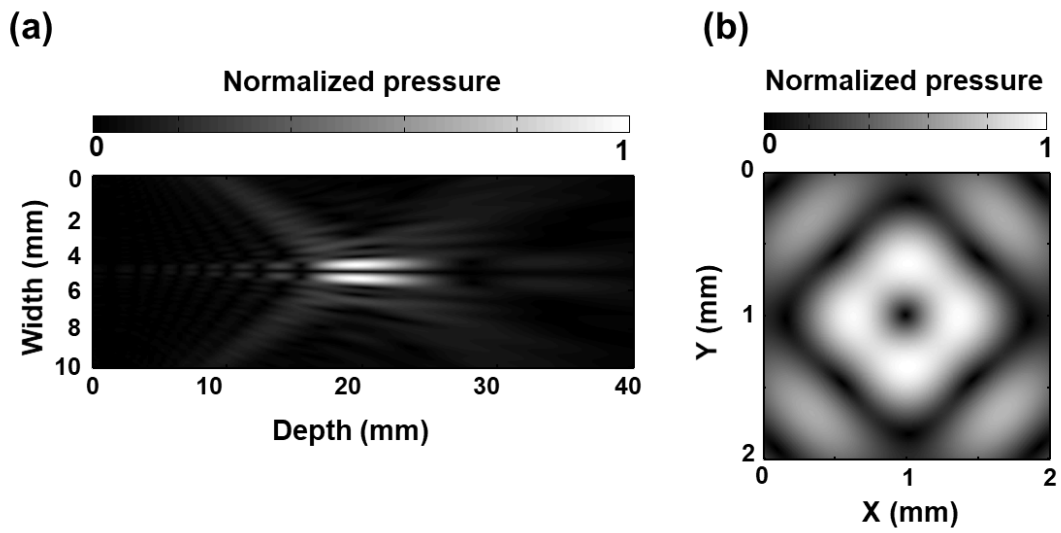

Fig. S1. The simulated data of designed transducer's focal length, the focal zone, and the beam width. (a) The pressure field along the direction of AVT propagation (x-z plane at y = 0 mm). **(b)** The transverse acoustic field at focal point (z = 20 mm).

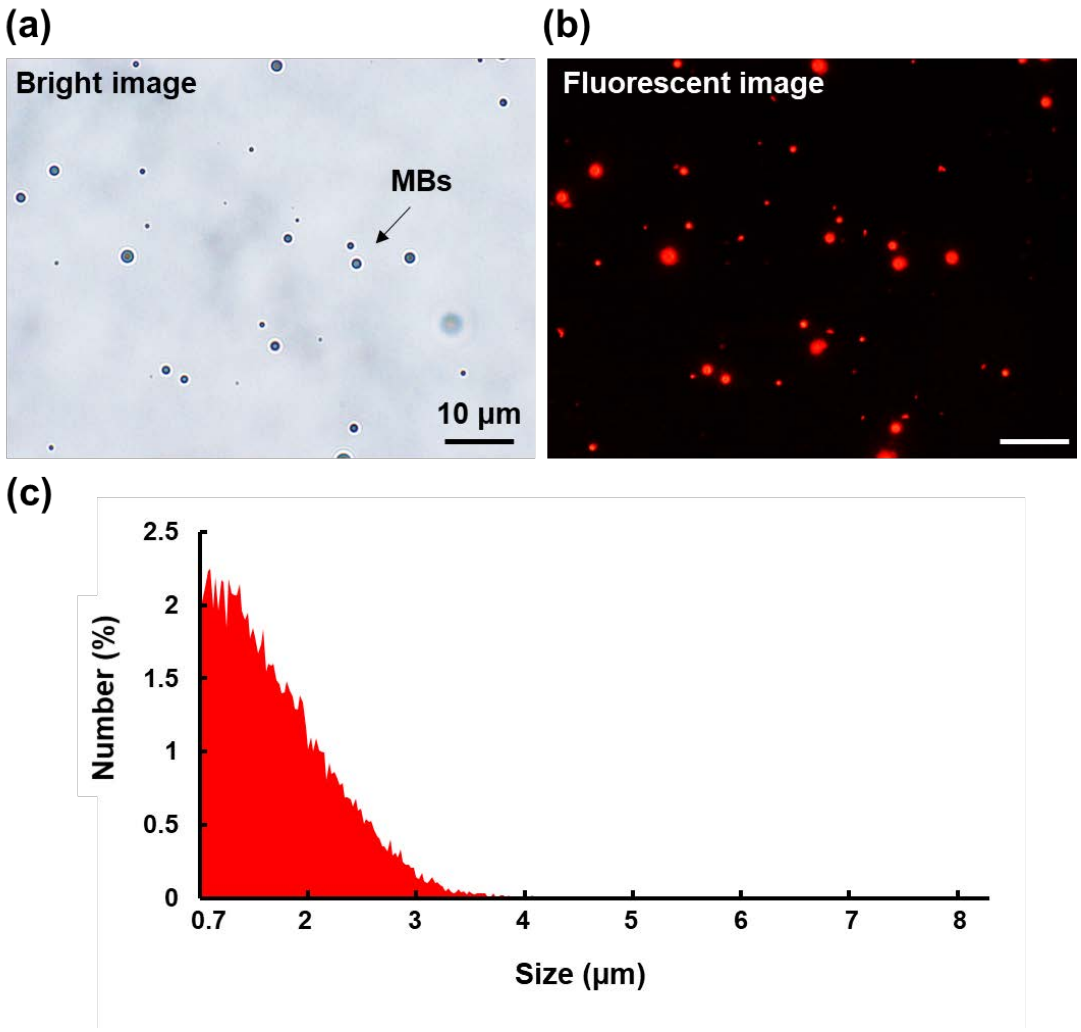

Fig. S2. The microscope images and size distribution of MBs. (a) The contours of MBs in bright field. **(b)** The fluorescent image of MBs. **(c)** A chart of MB size distribution shows mean radii of 1.1±0.5 μm.

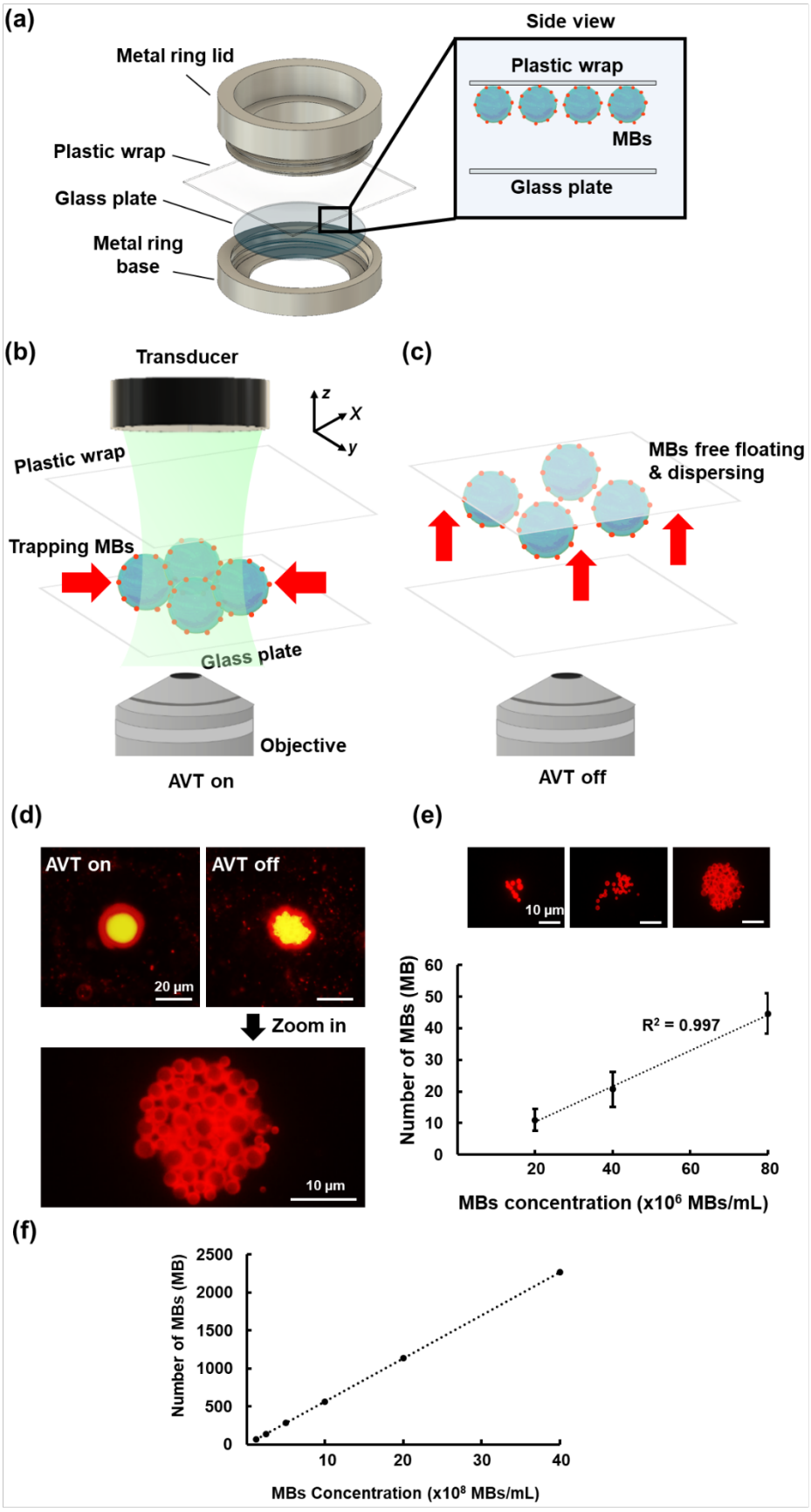
(a)
Side view
Metal ring lid
Plastic wrap
Glass plate
Metal ring base
Plastic wrap
MBs
Glass plate
(b)
Transducer
z
X
y
Plastic wrap
Trapping MBs
Glass plate
Objective
AVT on
(c)
MBs free floating & dispersing
AVT off
(d)
AVT on
AVT off
20 μm
Zoom in
10 μm
(e)
10 μm
Number of MBs (MB)
R² = 0.997
MBs concentration (x10⁶ MBs/mL)
(f)
Number of MBs (MB)
MBs Concentration (x10⁸ MBs/mL)

Fig. S3. In vitro experiment for estimating the number of AVT trapped MBs. (a) Experimental setup for counting the number of AVT-trapped MBs. **(b-c)** Experimental flowchart. The AVT-trapped MBs were released, and then waiting for natural dispersing. The number of MBs was counting under microscopic imaging. **(d)** The microscopic images during experiment. Following natural dispersing, the individual MB could be identified with 100× oil objective. **(e)** Top: the microscopic images of trapped MBs with different concentration (20, 40, and 80×10^6 MBs/mL); bottom: the corresponding number of MBs (1±3, 20±5, and 44±6). **(f)** The extrapolated number of MBs with high concentration (1.25, 2.5, 5, 10, 20 and 40×10^8 MBs/mL: 69, 140, 282, 566, 1133, and 2267).

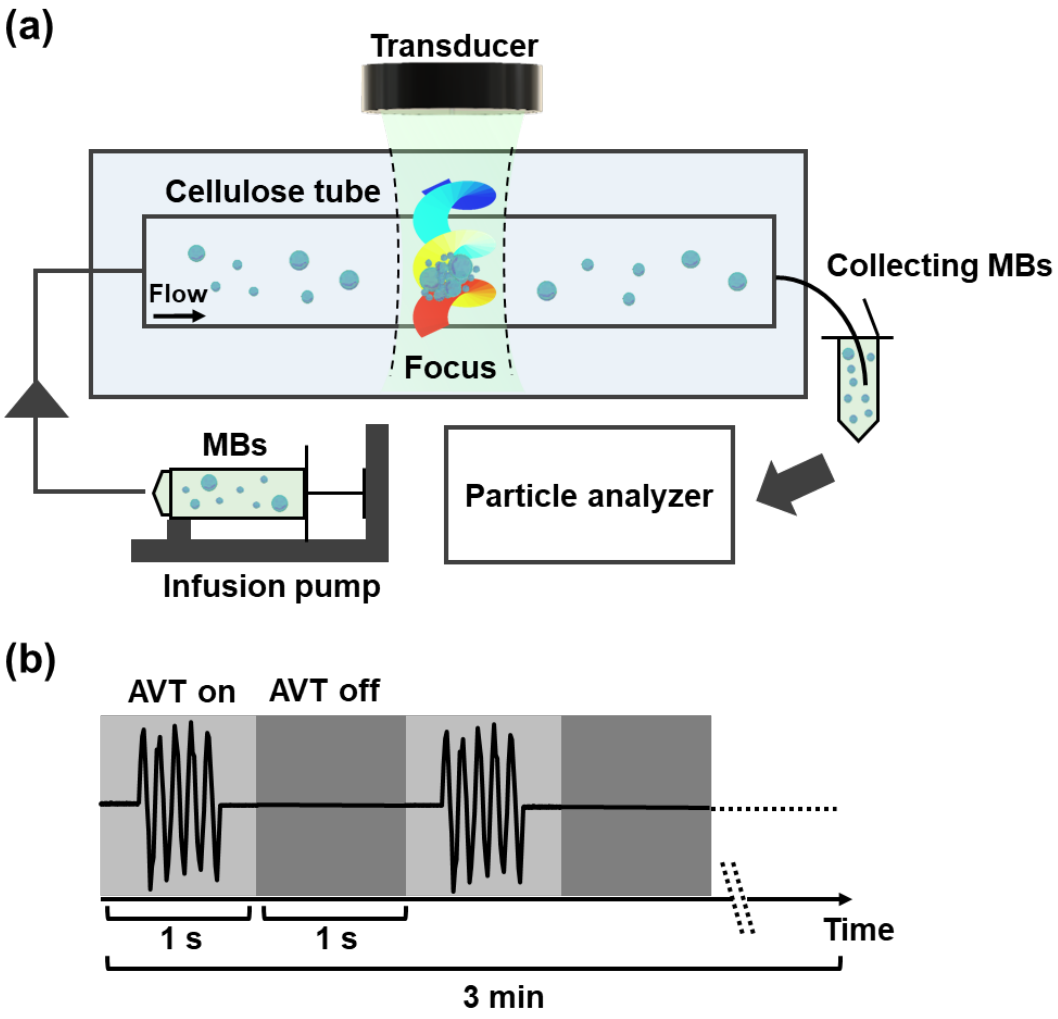

Fig. S4. Experiment to assess whether AVT trapping leads to MB clustering. (a) Illustration of experimental setup. **(b)** AVT trapping sequence. The AVT trapping was performed with MBs at a time interval of 1 s for 3 min.

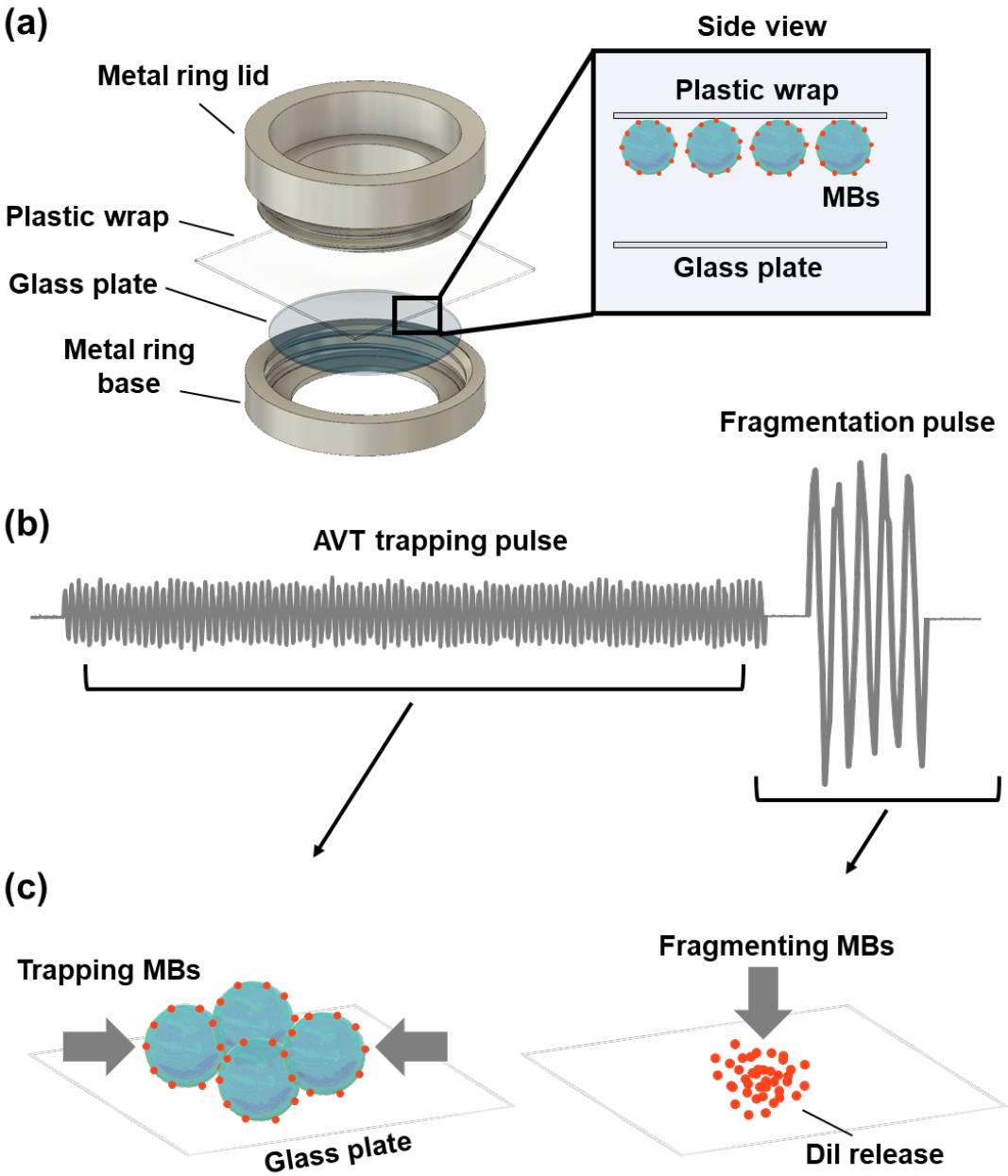

Fig. S5. Experiment of AVT trapping mediated drug delivery. (a) Experimental setup. **(b-c**) Schematic representation of AVT trapping-fragmentation sequence, showing the AVT trapping portion (left) and the fragmentation portion (right).

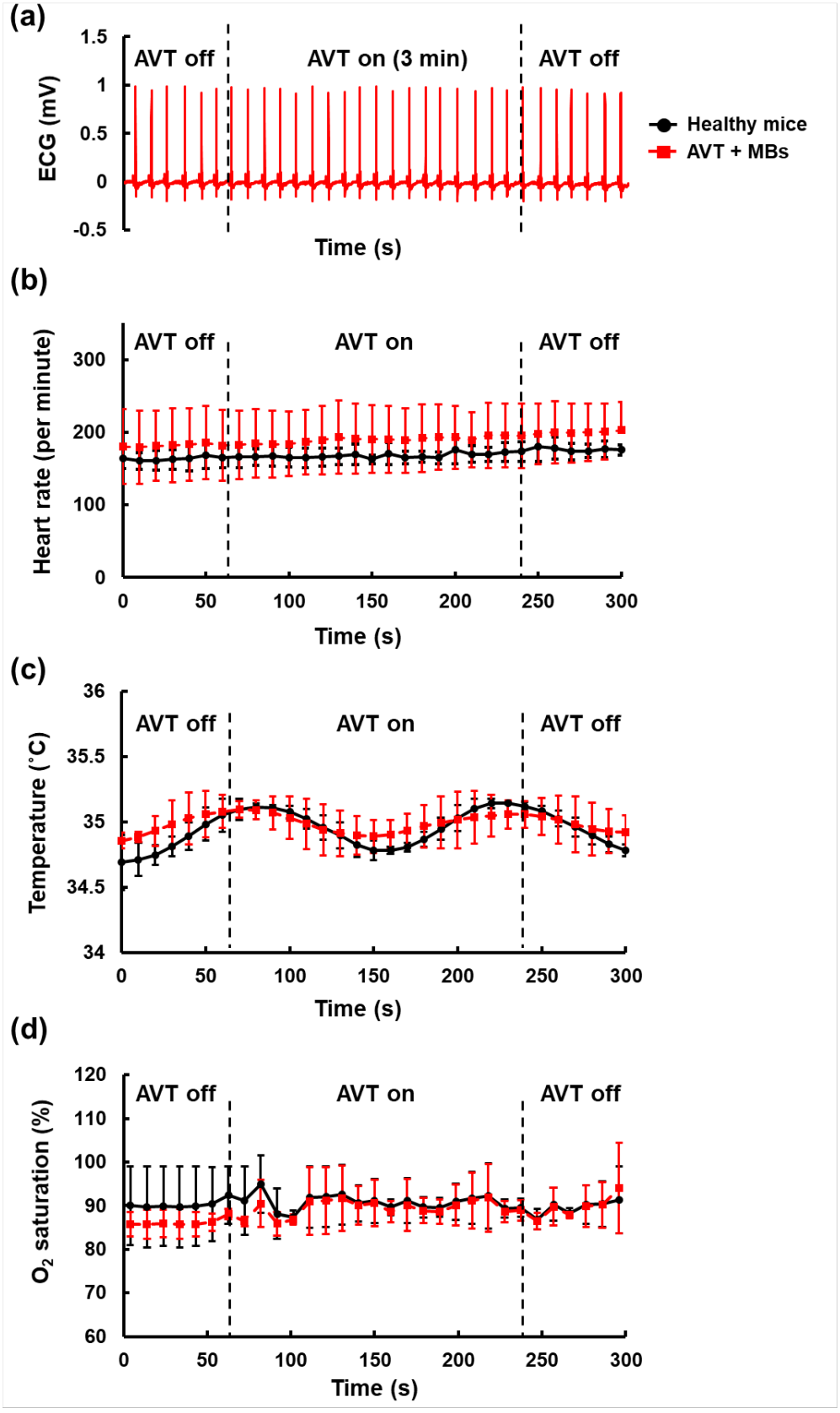
(a)
AVT off
AVT on (3 min)
AVT off
ECG (mV)
1.5
1
0.5
0
-0.5
Time (s)
Healthy mice
AVT + MBs
(b)
AVT off
AVT on
AVT off
Heart rate (per minute)
300
200
100
0
0
50
100
150
200
250
300
Time (s)
(c)
AVT off
AVT on
AVT off
Temperature (°C)
36
35.5
35
34.5
34
0
50
100
150
200
250
300
Time (s)
(d)
AVT off
AVT on
AVT off
O2 saturation (%)
120
110
100
90
80
70
60
0
50
100
150
200
250
300
Time (s)

Fig. S6. *In vivo* safety test of AVT trapping MBs. (a) ECG, **(b)** heart rate, **(c)** body temperature, and **(d)** blood oxygen concentration of mice before, during, and after receiving AVT-trapping MBs.

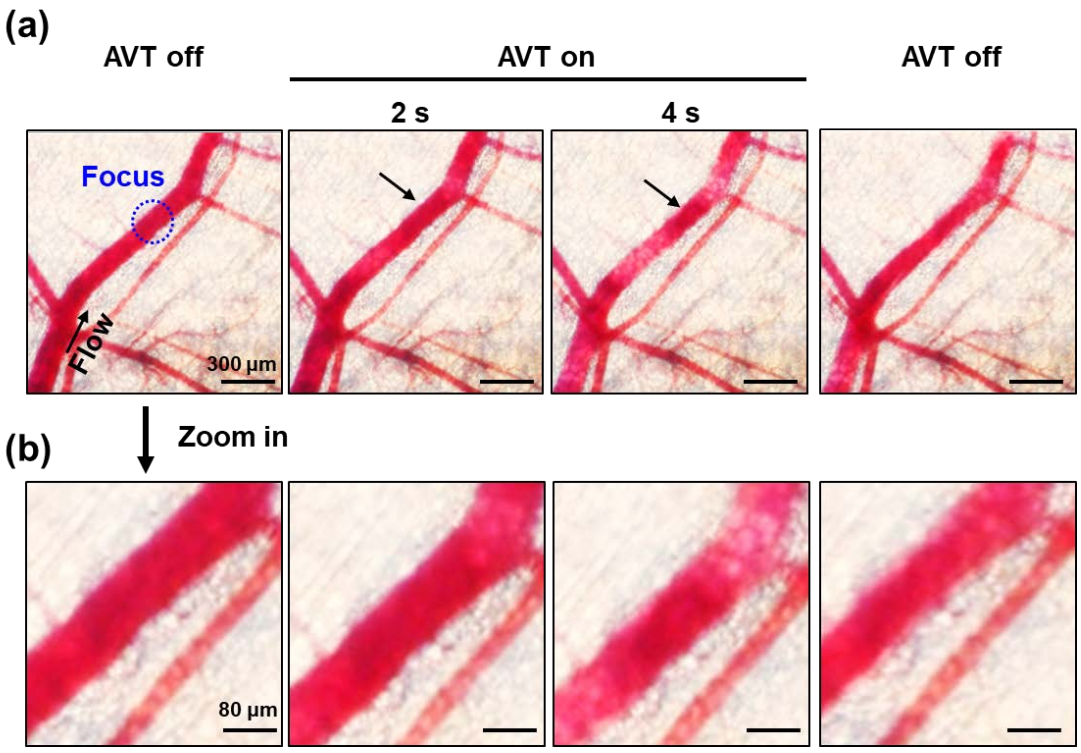

Fig. S7. Trapping RBCs by AVT *in vivo*. (a) The RBCs can be trapped at higher acoustic energy (800 kPa, 50% duty cycle) *in vivo*. **(b)** The magnification images show RBC trapping in the focal region of AVT.

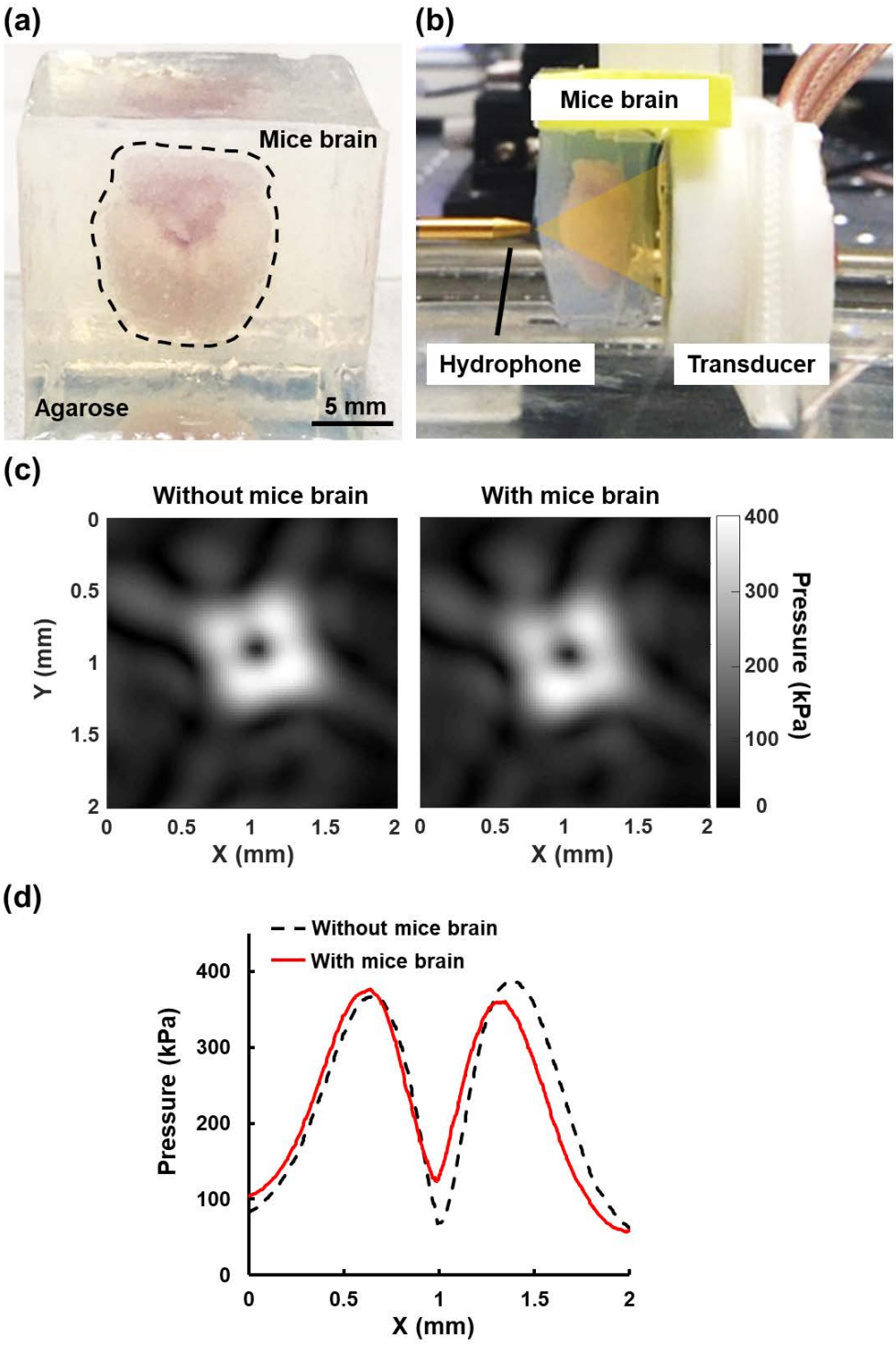

Fig. S8. Experiment for investigating whether the waveform of AVT is deformed as it passes through whole brain of mouse via a hydrophone. (a-b) Experimental setup. **(c)** Transverse pressure field measured at the focal point (z = 20 mm) with and without

penetrating the mouse brain, from which the ring pattern can be inferred from the vortex feature. **(d)** Comparison of the pressure fields in the lateral direction with and without penetrating mice brain. The pressure distribution shows that the formation of potential-well structure is not affected by brain tissue.

Legends for Movies S1 to S9

File Name: Movie S1 Description: Upon initiating the trapping, the aggregated MBs swirled around and ultimately became trapped in the center, thereby forming an MB cluster. Video is played at 15 fps.

File Name: Movie S2 Description: Series of side-view images showing that MBs initially experience the radiation force pushing on the wall and then the trapping force that immediately collects the dispersed clusters into the center of the AVT focal zone. Video is played at 15 fps.

File Name: Movie S3 Description: Zoomed-out view showing the formation of an upstream MB cluster during AVT initiation, which finally results in trapping failure. Video is played at 15 fps.

File Name: Movie S4 Description: The independent motion in the *x* and *y* directions by trapped MBs at a flow velocity of 2.6 cm/s. Video is played at 15 fps.

File Name: Movie S5 Description: Comparisons of AVT trapping in the presence of a mixture of MBs and pure blood in the static condition. Video is played at 15 fps.

File Name: Movie S6 Description: Comparisons of AVT trapping in the presence of a mixture of MBs and pure blood with flow velocity of 2.6 cm/s. Video is played at 15 fps.

File Name: Movie S7 Description: MB aggregation occurred when the AVT were trapping *in vivo*. Video is played at 15 fps.

File Name: Movie S8 Description: The MB cluster could be transversely moved from the centerline of the vessel to the vessel endothelium by adjusting the position of either the animal or the AVT transducer. Video is played at 15 fps.

File Name: Movie S9 Description: Although inflowing MBs accumulated upstream of the trapping zone, they started to disperse after passing the trapping zone. Video is played at 15 fps.

Reference

1. B. T. Hefner, P. L. Marston, An acoustical helicoidal wave transducer with applications for the alignment of ultrasonic and underwater systems. *J Acoust Soc Am* **106**, 3313-3316 (1999).
2. M. J. Shortencarier *et al.*, A method for radiation-force localized drug delivery using gas-filled lipospheres. *Ieee T Ultrason Ferr* **51**, 822-831 (2004).
3. https://standards.globalspec.com/std/10154661/ASTM%20F756